FULL-VALUE MAPPING OF GLACIER RHEOLOGY USING REPEAT PASS SAR INTERFEROGRAMS

Aleksey I. Sharov [(1)], Sven Etzold [(2)]

(1) Institute of Digital Image Processing, Joanneum Research, Wastiangasse 6, 8010 Graz, Austria
(2) Institute for Cartography, Dresden University of Technology, Mommenstrasse 13, 01062 Dresden, Germany

RESUME

An original phase gradient approach to glacier rheological modelling and mapping from repeat pass SAR interferograms was devised, programmed, tested and validated in different glacier environments. The underlying concept, basic algorithms, processional singularities and the information contents of our value-added interferometric products were analysed and briefly discussed. The technological efficiency and reliability of a new processing chain was proved by experiments on 14 ERS-1/2 spaceborne interferometric models. Several satellite image maps showing glacier dynamics in the Hintereisferner and Svartisen test sites were compiled, edited and printed at 1:50 000 and 1:100 000 scales. Map quality control was performed during special surveys in the field. The average tachometric accuracy of satellite rheological maps was estimated at ± 2.0 cm/day.

1 INTRODUCTION

The advancement of differential radar interferometry (DINSAR) in the 1990s established unprecedented technical capabilities for detecting and measuring the deformation and flow of glacier ice, and gave a strong impetus to the study of glacier rheology from space [1]. Numerous examples were already shown of successful DINSAR applications to studying three-dimensional flow of large glaciers, measuring short-term glacier velocities and identifying surge effects on ice fields. It has been demonstrated that the DINSAR method is applicable to precise rheological modelling in different glacial environments and that interferometric models of ice-surface rheology can be perfectly represented in the most versatile and easily interpreted form of satellite image maps [2, 3, 4].

Nevertheless, most research in the area is presently focussed on designing and validating algorithms for DINSAR data processing, while comparatively little attention is paid to appropriate cartographic representation of the glaciological information derived from interferometric surveys. This is quite evident from reviewing the interferometric maps of European glaciers published so far; most of them fall into the category of simple and hasty reproductions or provisional maps at best. Precise and elaborate DINSAR maps representing glacier dynamics in legible metrical form are still very few in number. This is presumably due to the algorithmic complexity of DINSAR and some uncertainties in the performance of this novel and somewhat unaccustomed technique making the involvement of traditional cartographic skills and expertise difficult [14, 15].

The present paper reports on the results and experience gained in producing detailed rheological maps through the use of repeat-pass interferometric SAR data obtained from ERS-1/2 satellites over large European glacial areas including Hintereisferner, a typical valley glacier in the Austrian Alps with a long history of surveys, and the Svartisen Ice Caps in Northern Norway, an important site for hydropower production. An original and stringent albeit very simple algorithm has been applied to the reconstruction of glacier rheology from interferometric phase gradients (GINSAR) that does not involve complex process artifices, does not require accurate reference topographic models and provides fast, global and reliable solutions for reliable mapping of glacier dynamics in various environments.

An experimental data set included all necessary Austrian and Norwegian topographic maps, multitemporal records documenting the rate of glacier ice flow and 7 pairs of ERS-1/2 SAR interferograms taken under steady and cold weather conditions in 1995/96, which were processed with the RSG 4.6 software package. Cartographic styling, drafting, scribing and editing were performed using the ArcInfo 8.1 and FreeHand 10 software. Some developments in cartographic design and symbolisation contributed their share to the aesthetic appearance of map sheets. As a result 3 combined map sheets showing the distribution of the glacier strain rate, ice velocities and glacier marginal changes in both test sites at different scales ranging from 1:25 000 to 1:100 000 were compiled, printed and verified on a cost-effective basis, thus completing the whole processing chain.

2 METHOD

The idea of proceeding from operations on original (wrapped) SAR interferograms to the analysis of their derivatives or phase gradients set up a solid methodological base for the unsupervised detection of glacier changes and the spatial reconstruction of glacial flow from repeat pass INSAR data. In our GINSAR approach, interferometric phase gradients ($\nabla\varphi_x$ and $\nabla\varphi_y$) are calculated in the image domain simply by subtracting the original interferential picture from a shifted version of the same picture as an ortho- or cross-gradient:

$$\overset{+}{\nabla}\varphi(x,y) = \nabla\varphi_x(x,y) + \nabla\varphi_y(x,y) \cong \left|\varphi(x+1,y) - \varphi(x,y)\right| + \left|\varphi(x,y+1) - \varphi(x,y)\right|;$$
$$\overset{\times}{\nabla}\varphi(x,y) \cong \left|\varphi(x+1,y+1) - \varphi(x,y)\right| + \left|\varphi(x,y+1) - \varphi(x+1,y)\right|. \quad \textbf{(1)}$$

Both procedures are very simple, and the results appear to be highly satisfactory; instead of a striped interferential picture we obtain a continuous picture, which provides a realistic view of the steady terrain and is called *a topogram*. The topogram, e.g. that in Fig. 1 showing Fingerbreen Outlet Glacier in the Svartisen test site, is more legible for an average reader than the original picture. In modern remote sensing you do not often find such a situation.

The shift values $\delta(x,y)$ are usually equal to 1 pixel (as in Eq. 1), but, in general, can be manipulated separately in azimuth (x) and range (y) direction within the interval from 0 to several pixels. Further increase in the shift value coarsens the spatial resolution of the topogram.

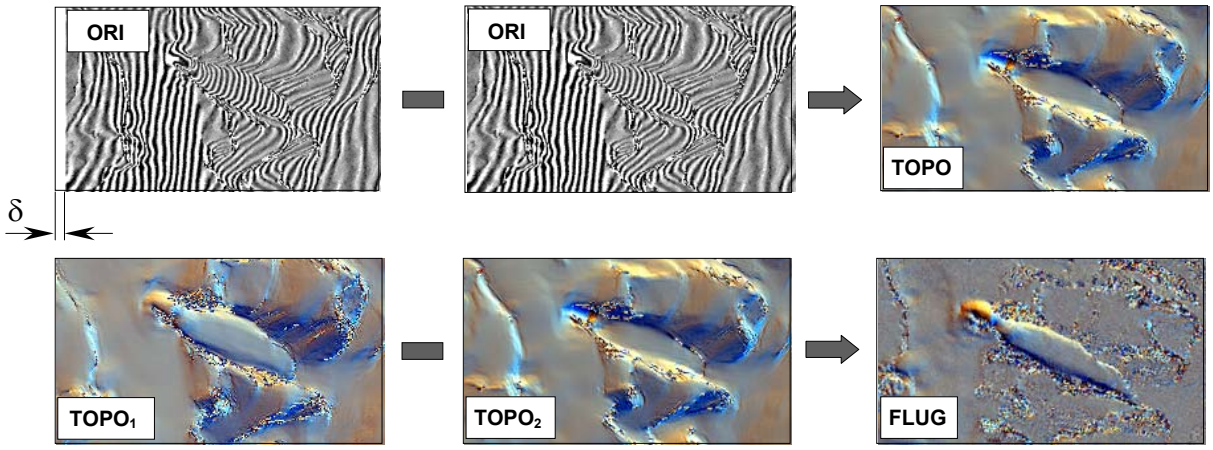

Fig. 1. Underlying concept of the GINSAR method

In the interferential picture of an active glacier, the rate of motion fringes is usually much higher than that of topographic fringes and the differentiation procedure attenuates the topographic component partly or completely and emphasises the motion phase. In cases of flat glacial topography, local quantitative analysis of ice motion can thus be performed even in single topograms [15]. Accurate processing of the repeat-pass SAR interferograms with large spatial baselines obtained over steeper glaciers requires the impacts of surface topography and surface displacement on the interferometric phase to be fully separated. If the glacier topography is supposed to be unchanged between subsequent INSAR surveys, its contribution to the interferometric phase can be excluded by differencing between two co-registered multitemporal topograms of the same glacier. In order to account for differences in surveying geometry, each of the topograms is *geocoded* beforehand and *scaled* with a real, not necessarily integer scaling factor

$$C(x,y) = 0.25\pi^{-1} \cdot \lambda \cdot B_{\perp}^{-1}(x) \cdot R(y) \cdot \sin\theta(y) \quad \text{[m]}, \quad \textbf{(2)}$$

where $\lambda = 0.0566$ m is the SAR wavelength, $B_{\perp}(x)$ is the length of the perpendicular component of the baseline, $R(y)$ - the slant range, $\theta(y)$ - the look angle.

Assuming that $\nabla\varphi = \nabla\varphi_{topo} + \nabla\varphi_{mot}$ and $C_1 \cdot \nabla\varphi_{topo\,1} = C_2 \cdot \nabla\varphi_{topo\,2}$, the operation of differencing between two scaled multitemporal topograms can be formulated as follows

$$F = C_1 \cdot \nabla\varphi_1 - C_2 \cdot \nabla\varphi_2 = C_1 \cdot \nabla\varphi_{mot1} - C_2 \cdot \nabla\varphi_{mot2}\,, \qquad \textbf{(3)}$$

and the resultant *fluxogram F* contains only the differential motion phase without topographic phase. In the fluxogram, objects undergoing temporal changes / motions, e.g. the active tongue of Fingerbreen, can be clearly distinguished and delineated from those tracts of land or ice that did not change / move between INSAR surveys and appear completely flat, e.g. an area eastward from Fingerbreen (Fig. 1). In our fluxograms, pixel values have the dimensions of length [m].

In order to solve the basic differential equation (3) with regard to one of motion phase gradients, e.g. $\nabla\varphi_{mot1}$, we assume that the relation between ice-velocity gradients remains constant over the time span covered by both interferograms, i.e.

$$a = \nabla\varphi_{mot2} / \nabla\varphi_{mot1} = const\,. \qquad \textbf{(4)}$$

This *steady flow assumption* proved to be more reliable in our test glacial areas than the traditional constant velocity constraint[1]. The parameter *a* can be determined from available ground-truth data or derived from single SAR interferograms on the basis of the transferential approach described in [14]. Alternatively, reference values for the parameter *a* can be obtained from conventional 2-pass DINSAR products. The limited accuracy of the reference interferograms simulated from available DEMs is not very critical in this case. If parameter *a* is known, then the fluxogram can be directly converted to a new image product using the following relation

$$\nabla\varphi_{mot\,1} = F \cdot (C_1 - aC_2)^{-1} = 4\pi \cdot \Delta V_1 \cdot T_1 \cdot \lambda^{-1}\,, \qquad \textbf{(5)}$$

where ΔV_1 is the velocity gradient in the first interferogram. An image product of this kind provides relative information about the glacier motion variations and can be used for the analysis of the glacier strain rate; the latter is calculated as a difference between two neighbouring velocity values divided by the distance between velocity records *Δp*, i.e.

$$S = \Delta V / \Delta p = b \cdot p^{-1} \cdot T^{-1} \cdot F \cdot (C_1 - aC_2)^{-1} \quad [\text{day}^{-1}], \qquad \textbf{(6)}$$

where coefficient b equals $0.25\lambda/\pi$ for the longitudinal strain and $0.125\lambda/\pi$ for the share strain rate; T = 1 day for INSAR tandem surveys; p is the interferometric pixel size on the ground in [m].

The idea of calculating both the longitudinal and the share strain rates in a straightforward manner from motion phase gradients is more or less new, because almost all researchers working in the area of glacier interferometry determine the glacier velocity first and only then calculate the strain rate from the velocity values, c.f. [5]. A high strain rate value indicates the possible occurrence of crevasses on the glacier surface, which represent a serious hazard for hikers. During field surveys on Western Svartisen in 2002 we revealed several *buried* crevasses near the ice divide; their location coincided with local maximum values of the strain rate in the image product *S*. Recently, we revealed that more than 70% of all "stressed" areas at glacier margins manifested in the strain-rate image product (STRIP) of 1996 later on underwent essential retreat or advance as shown in our maps of glacier marginal changes from 2003. We still do not know whether high glacier strain rate values might reliably indicate future surficial changes in the glacier interior.

Scaled fluxograms (Eq. 5) were successfully applied to measuring glacier velocity values along the line-of-sight direction by integrating motion phase gradients. In our case, glacier velocities were determined by applying the

[1] Our experience shows that the steady flow assumption is not always valid, especially under long temporal intervals *ΔT* between topograms and sufficiently fast ice flow when the amount of glacier motion exceeds the interferometric pixel size on the ground [16]. Such cases requiring *"wave flow assumption"* and relevant methods of feature / coherence tracking are treated in other publications [14, 6].

Cholesky algorithm to solving an over-determined system of linear equations, which relate the unknown velocities with their gradual observations in a least-square manner [16]. The procedure was carried out only over moving areas, which were delineated in the fluxogram, thus excluding steady areas from the analysis, reducing the computational load and diminishing the areal error propagation. The integration product representing the spatial distribution of ice velocities, yet without showing the motion direction, is called *a velogram*.

In general, the surface flow direction can be estimated in three dimensions by using dual-azimuth processing of multitemporal SAR topograms obtained from opposite, i.e. ascending and descending orbits [7]. In the Hintereisferner test site, this method could not be applied, however, because of the significant layover effect masking the glacier surface in all descending scenes. In the Svartisen test site, this approach did not bring an essential gain due to the "favourable" orientation of the test outlet glaciers mostly coinciding with the SAR range direction for descending orbits and insignificant values of the short-term vertical motion component derived from the winter INSAR pairs. We thus confined our work to processing the INSAR data obtained from parallel orbits assuming the glacier flow to be parallel to the ice surface, normal to topographic contours and parallel to glacier walls / flanks. After decomposing, attributing and editing our velograms were transformed into the image-based rheological maps presented in the next chapter.

3 MAPS

Satellite image maps presenting all surface details in their real appearance with the addition of conventional graphic elements are ideal for depicting glacial areas, where natural features are predominant, complicated socio-economic objects are scarce, and vegetation cover is negligible [13]. They can be produced relatively quickly and at low cost, if done on a standard PC. Practical mapping of glacier rheology in our test sites was performed on the basis of a combined technology using software tools for data compilation / assimilation, cartographic design, computer graphics and GIS. The principal stages of our mapping technology and the software used are presented in Fig. 2.

All input GINSAR products (topograms, fluxograms, strips and velograms) are represented in the form of an RGB image. The first two layers represent *partial* phase gradients or their derivates in azimuth (x) and range (y) direction, while the third layer gives the *full* two-dimensional phase derivative showing the absolute values of related parameters. Correspondingly, the whole cartographic information to be placed on the *digital* map was organised in different layers: three image (raster) layers and several graphic (vector) layers, one containing the contour lines and glacier borders, one including textual information in vector format and the other depicting all remaining graphic features. In order to legibly depict the information from several raster layers on a *paper* map we applied the principle of continuous two-dimensional colour representation known as **IHS** colour system using the combination of visual variables "hue" and "value" (saturation and intensity) for the representation of any point (or vector) in the x, y domain. For the sake of illustration, Fig. 3 shows a small fragment from the legend for our strain rate maps.

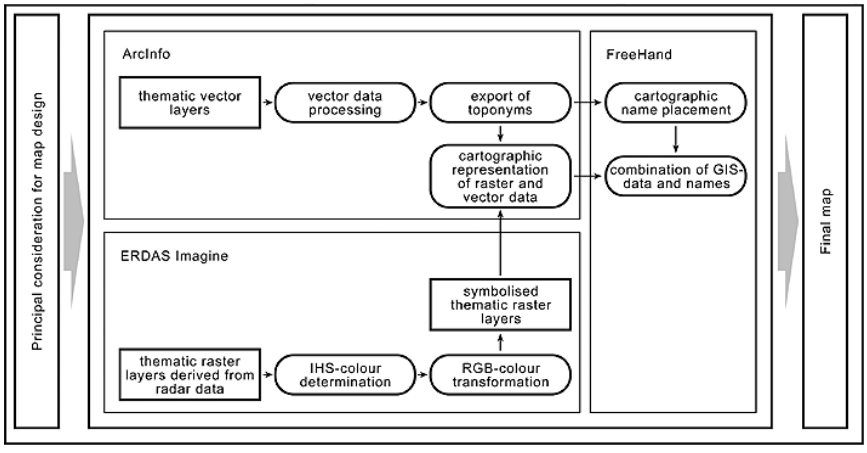

Fig. 2. Cartographic workflow

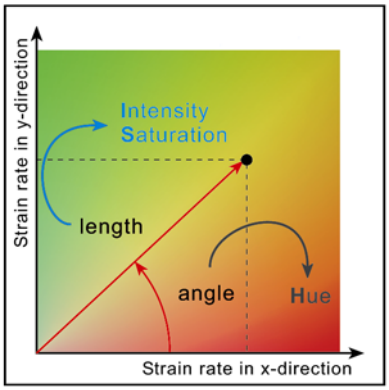

Fig. 3. Representation of the glacier strain rate using IHS-colour system

Topographic 1:50 000 maps issued by Austrian (ÖK-50 in Gauss-Krüger projection, Bessel ellipsoid) and Norwegian (M711 in UTM projection, WGS84 ellipsoid) national surveys in the 1990s provided the necessary topographic information and served as a geometric base (cartographic projection, geographic grid, accuracy standards) for our rheological maps. Map scale and contour interval (50 m, equidistant for all maps) were determined in accordance with the project specifications and standard requirements for the information contents of satellite image maps [8, 9]. All toponyms were given in national transcriptions, while map legends, mastheads and imprints were in English. In ArcInfo 8.1, the automatic placement of cartographic names, spot elevations and contour values did not work properly, which is why the final placement was verified and edited manually in FreeHand 10.

As a result, 12 satellite rheological maps were compiled, verified and edited, including

- an overview map showing the distribution of glacier strain rate in the Svartisen area at 1:100 000 scale,
- eight detailed maps showing ice velocities and glacier marginal changes at Engabreen, Fingerbreen, Frukostindenbreen and Storglombreen outlet glaciers in the Svartisen test site, each at 1:50 000 scale,
- two maps of the glacier strain rate and glacier velocities in the Hintereisferner test site at 1:50 000 scale,
- an auxiliary map showing glacier marginal changes in the Hintereisferner test site at 1:25 000 scale.

These maps were arranged in 3 thematic groups according to their information contents and printed together on 3 combined A2 map sheets. Their small-size copies are shown in Fig. 4.

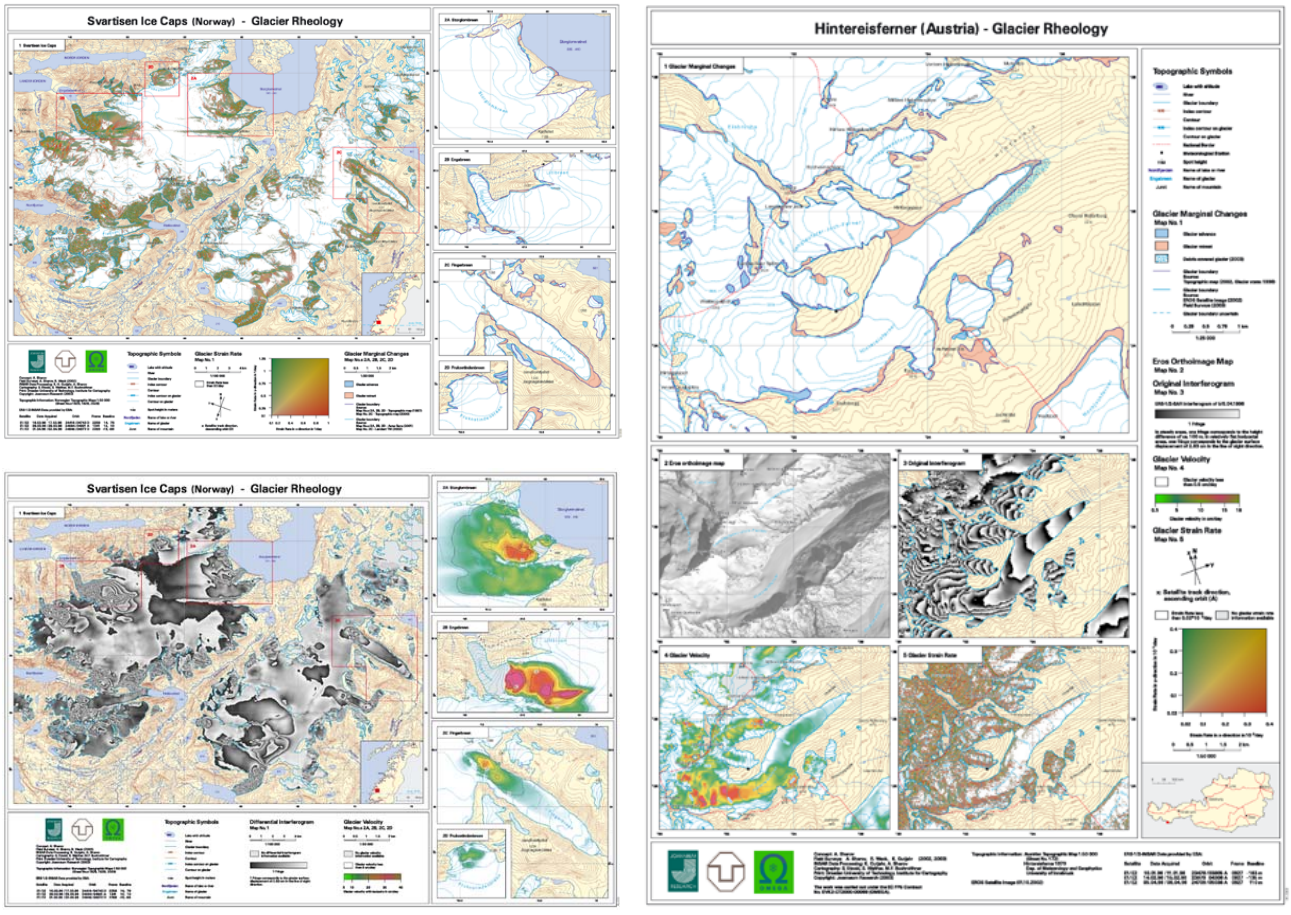

Fig. 4. Satellite rheological image maps of Svartisen Ice Caps, Northern Norway (on the left) and Hintereisferner Glacier, Oetztal Alps (on the right).

4 ACCURACY

Tachometric map substitutes published recently by Austrian [10] and Norwegian [11] colleagues were used for the first checks of our rheological models. In the Svartisen test site, the mean difference between the geodetic and GINSAR velocities at 11 checkpoints was – 0.5 cm/day and the r.m.s. difference was given as ± 2.25 cm/day. In the Hintereisferner test site, the absolute differences in glacier velocities reached 40% although the flow patterns were relatively similar and consistent.

Map quality control and content review was further performed in 2002 and 2003 during terrestrial surveys and observations using high-precision geodetic equipment and different surveying techniques such as DGPS, tacheometry, forward intersection, automatic tracking, terrestrial photogrammetry and laser scanning. In total, we carried out nearly 2000 precise terrestrial tachometric measurements in 3 to 5 periods, involving 70 target points on 9 different glaciers. Average annual horizontal velocities of Hintereisferner Glacier at altitudes ranging from 2560 to 2920 m a.s.l. and corresponding velocities obtained by the GINSAR and conventional 2-pass DINSAR techniques are graphically shown in Fig. 5. The glacier velocities surveyed in the field were generally consistent with both the GINSAR and 2-pass DINSAR values, although the GINSAR values were far less scattered. One can see, however, that there is a systematic difference of about +5.0 cm/day between the interferometric velocities and those from field surveys.

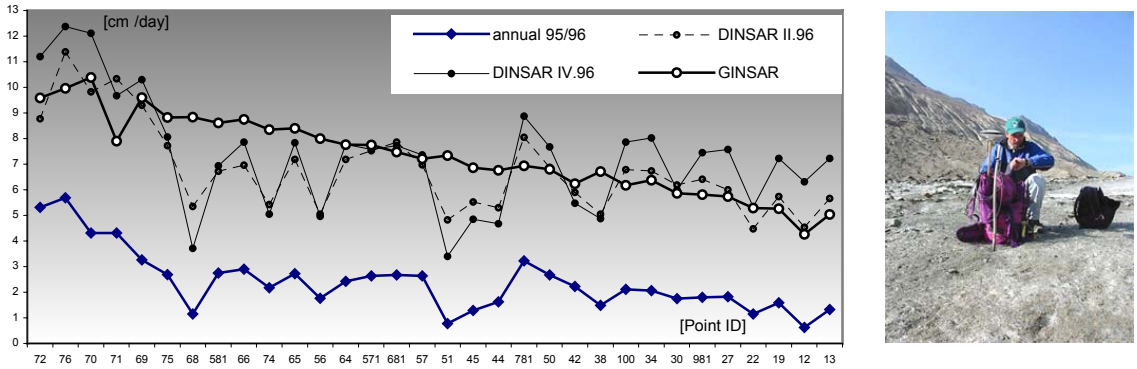

Fig. 5. Interferometric velocities (cm/day) versus average annual velocities 1995/96 on Hintereisferner Glacier.

We thus matched and adjusted the velocity values obtained from independent and redundant terrestrial and interferometric surveys over 43 tie points in a manner similar to that used for height values in stereophotogrammetric geocoding. In contrast to traditional scaling procedures established in glacier interferometry, we excluded tie points with zero velocities from the analysis, and used them only for ancillary control. The procedure of simple *linear* adjustment applied to the GINSAR models reduced the mean difference between interferometric and field velocities to +0.23 cm/day and resulted in an estimated r.m.s. difference of ± 1.9 cm/day. In this respect, the interferometric velocities and rheological maps obtained by our GINSAR method in both test sites can be interpreted as being quite accurate. This being said, the impact of seasonal changes in glacier motion and the influence of INSAR undersampling in fast moving areas at larger glacier slopes or undulations on the tachometric accuracy must still be investigated.

It is at all events worth noting that the information contents of traditional tachometric maps are inferior to those of GINSAR models, e.g. in detecting ice deformations and measuring ice-surface velocities in hard-to-reach locations as well as in determining the actual position of glacier termini if the glacier surface is covered with snow or debris. Our rheological maps proved to be invaluable both in the detailed planning of field campaigns and in the identification of various surface features, slope effects and other critical areas for which ground information was needed. In order to account for slope effects and to improve the general methodological performance, we recently reviewed our GINSAR flow chart and introduced new procedures of normalising phase gradients and generating slope maps from topograms. There are still several unresolved questions and opportunities for further technological improvements, e.g. those related with the somewhat complicated interpretation of "static" interferometric models and proceeding to dynamic representations / animations of glacier changes. The usage of "scalable vector graphics" mentioned in [12] is considered to be very promising in this context.

5 CONCLUSIONS

High metric quality and detail, consistent and complementary information contents, proportionally long legends, conformity with available standards, attractive appearance and the wide range of possible applications provide ample proof that our satellite rheological maps are to be regarded as full-value cartographic products. Our interferometric models represented in the most complete, albeit concise and easily interpreted form are deemed to demonstrate clearly the functional quality and processional advantages of a new GINSAR technology ideally suited for automated glacier cartography.

The GINSAR method mitigated serious processional drawbacks related to the operation of interferometric phase unwrapping, thus reducing processing time and improving mapping accuracy. In contrast to traditional DINSAR, our approach utilises less stringent and more reliable assumptions about the character of glacier motion, and, in cases of relatively flat glacial topography, local quantitative analysis of ice flow can be performed even in single interferograms. The approach preserved the ground resolution of original interferograms and, despite some initial doubts, did not increase the phase noise notably. The GINSAR algorithm was implemented in the new RSG 4.6 software package distributed by Joanneum Research. 14 GINSAR models have already been processed, checked and validated, and all the results were entirely consistent and satisfactory.

New output interferometric products such as topograms, fluxograms, strain rate image products, glacier slope maps (in steady areas), and rheological maps can be applied to solving various glaciological tasks in different environments, irrespective of the kind and source of interferometric scenes. The average tachometric accuracy of satellite rheological maps for the Hintereisferner and Svartisen test sites was estimated at ± 2.0 cm/day. We are currently looking for additional interferometric and ground-truth data and believe that new operational and upcoming spaceborne SAR systems such as ENVISAT and CRYOSAT and their possible "tandem use" could provide a great incentive for glacier interferometry in general and our further work in particular.

ACKNOWLEDGEMENTS

The present research was carried out under the EC FP5 Contract No. EVK2-CT2000-00069 (OMEGA). The ERS-1/2-INSAR data for our studies were generously provided by ESA. The authors offer their sincere thanks to all the colleagues who supported this work and took part in valuable discussions.

REFERENCES

1. Goldstein R., Engelhard R., Kamb B., and Frolich R. Satellite radar interferometry for monitoring ice sheet motion: application to an Antarctic ice stream. *Science*, **262**, 1525-1530, 1993.
2. Joughin I. *et al*. Ice flow of Humboldt, Petermann, and Ryder Gletscher, northern Greenland. *J.Glac.,* **45** (150), 231-241, 1999.
3. Forster R. *et al.* Interferometric radar observations of Glaciers Europe and Penguin. *J.Glac.,* **45** (150), 325-336, 1999.
4. Murdock M. First ever maps of Antarctic ice movement created from radar interferometry. IEEE G&RS Society Newsletter, 6-9, June 2001.
5. Rack W. *et al.* Interferometric analysis of the deformation pattern of the northern Larsen Ice Shelf, Antarctic Peninsula, compared to field measurements and numerical modelling. *Annals of Glaciology*, **31**, 205-210, 2000.
6. Strozzi T., Luckman A., Murray T., Wegmüller U., and Werner C. Glacier motion estimation using SAR offset-tracking procedures. *IEEE Geoscience and Remote Sensing*, **40**(11), 2384-2391, 2002.
7. Joughin I., Kwok R., and Fahnestock M. Interferometric estimation of three-dimensional ice-flow using ascending and descending passes. *IEEE Trans. Geosc. &RS*, **36** (1), 25-37, 1998.
8. Colvocoresses A.P. Image Mapping with the Thematic Mapper. *Photogrammetric Engineering and Remote Sensing*, **52**, 1499-1505, 1986.
9. Koch, W.G. Minimaldimensionen in der Kartographie, in: Bollmann, J., W.G. Koch (eds.), *Lexikon der Kartographie und Geomatik*, Heidelberg, 2002.
10. Nagler T., Mayer C., Rott H. Feasibility of DINSAR for mapping complex motion fields of Alpine ice- and rock-glaciers. Proc. 3d Int. Symp."Retrieval of Bio- and Geophysical Parameters from SAR Data". Sheffield, UK, 377 –382, 2002.
11. Kjöllmoen B. (Ed.), "Glaciological investigations in Norway in 2001". NVE Report **1**, 102 p., 2003.
12. Kääb A. et al. Glaziale und periglaziale Prozesse: Von der statischen zur dynamischen Visualisierung. *Kartographische Nachrichten*, **5**, 206-212, 2003.
13. Sharov A.I. Practical application of satellite phototopography to mapping tasks in Franz Josef Land. *Petermanns Geographische Mitteilungen* **293**, 57-82, 1997.
14. Sharov A.I., Glazovskiy A.F. and Meyer F. Survey of glacial dynamics in Novaya Zemlya using satellite radar interferometry. *Zeitschrift für Gletscherkunde und Glazialgeologie,* **38**, 1-19, 2003.
15. Sharov A.I., Gutjahr K., Pellikka P.E. Phase gradient approach to the evaluation and mapping of glacier rheology from multi-pass SAR interferograms. Proc. 2d Int. Workshop «Multitemp 2003», July 16-18, 2003, JRC, Ispra, Italy, 11 p. (in print).
16. Sharov A.I., Gutjahr K., Meyer F. and Schardt M. Methodical alternatives to the glacier motion measurement from differential SAR interferometry. *IAPRS*, **XXXIV**, 3A, 324 – 329, 2002.